JCI insight

RESEARCH ARTICLE

T cell Bim levels reflect responses to anti–PD-1 cancer therapy

Roxana S. Dronca,[1] Xin Liu,[2] Susan M. Harrington,[3] Lingling Chen,[2] Siyu Cao,[2] Lisa A. Kottschade,[1] Robert R. McWilliams,[1] Matthew S. Block,[1] Wendy K. Nevala,[4] Michael A. Thompson,[4] Aaron S. Mansfield,[1] Sean S. Park,[5] Svetomir N. Markovic,[2,4] and Haidong Dong[2,3]

[1]Division of Medical Oncology, [2]Department of Immunology, [3]Department of Urology, [4]Division of Hematology, and [5]Division of Radiation Oncology, Mayo Clinic, Rochester, Minnesota, USA.

Immune checkpoint therapy with PD-1 blockade has emerged as an effective therapy for many advanced cancers; however, only a small fraction of patients achieve durable responses. To date, there is no validated blood-based means of predicting the response to PD-1 blockade. We report that Bim is a downstream signaling molecule of the PD-1 pathway, and its detection in T cells is significantly associated with expression of PD-1 and effector T cell markers. High levels of Bim in circulating tumor-reactive ($PD\text{-}1^{+}CD11a^{hi}CD8^{+}$) T cells were prognostic of poor survival in patients with metastatic melanoma who did not receive anti–PD-1 therapy and were also predictive of clinical benefit in patients with metastatic melanoma who were treated with anti–PD-1 therapy. Moreover, this circulating tumor-reactive T cell population significantly decreased after successful anti–PD-1 therapy. Our study supports a crucial role of Bim in both T cell activation and apoptosis as regulated by PD-1 and PD-L1 interactions in effector $CD8^{+}$ T cells. Measurement of Bim levels in circulating T cells of patients with cancer may provide a less invasive strategy to predict and monitor responses to anti–PD-1 therapy, although future prospective analyses are needed to validate its utility.

Introduction

The programmed death 1 (PD-1) pathway has been found to play a crucial role in tumor-induced immunosuppression in melanoma, lung cancer, renal cell cancer, and other malignancies and is an increasingly exploited therapeutic target (1–6). PD-1 blockade aims to restore antitumor immunity by impeding interactions of the PD-1 receptor expressed by tumor-reactive T cells with PD-1 ligands (e.g., PD-L1/B7-H1/CD274) expressed by tumor cells (7, 8). Clinical trials with PD-1 and PD-L1 blockade have demonstrated promising therapeutic responses in patients with advanced malignancies, including melanoma (1–3, 6). Recently, two anti–PD-1 monoclonal antibodies (pembrolizumab and nivolumab) have been approved by the US FDA for the treatment of patients with metastatic melanoma (MM) and metastatic non–small-cell lung cancer, and nivolumab was also approved to treat patients with advanced (metastatic) renal cell carcinoma (3–5, 9). However, clinical outcomes with immune checkpoint agents remain quite variable, with some patients achieving durable responses, others experiencing early disease progression followed by later tumor reduction, and some showing no benefit (1, 3). In addition, radiologic responses are often unpredictable, kinetically heterogeneous, and do not follow traditional response criteria. Analysis of the time to response to pembrolizumab in reported clinical trials indicates that, although most responses occur by week 12, some responses may also occur late in the course of treatment and were observed as late as 36 weeks (10). In addition, 8% to 10% of patients experienced pseudoprogression, with a ≥25% increase in tumor burden that was not confirmed as progressive disease on subsequent imaging, and these patients still had favorable clinical outcomes (10, 11). Because of the unconventional response patterns seen with immunotherapeutic agents, alternative methods of evaluating tumor response/progression have been implemented, including the immune-related response criteria (12) and the practice of confirming disease progression on subsequent scans, provided that the patient is clinically stable and maintaining a good performance status. Nevertheless, it is unclear what ultimately separates responders from nonresponders, and there are no definitive criteria by which to identify patients who may ultimately benefit from these immunotherapies. In addition, the optimal duration of therapy with PD-1 pathway blocking agents remains yet to be determined.

Authorship note: S.N. Markovic and H. Dong are co–senior authors.

Conflict of interest: H. Dong and S.N. Markovic are inventors of US patent 9302005 B2, Method and materials for treating cancers. H. Dong, S.M. Harrington, and X. Liu are inventors of US patent application WO2015050663A1, Methods for treating cancer in patients with elevated levels of Bim.

Submitted: December 11, 2015
Accepted: March 29, 2016
Published: May 5, 2016

Reference information:
JCI Insight. 2016;1(6):e86014.
doi:10.1172/jci.insight.86014.

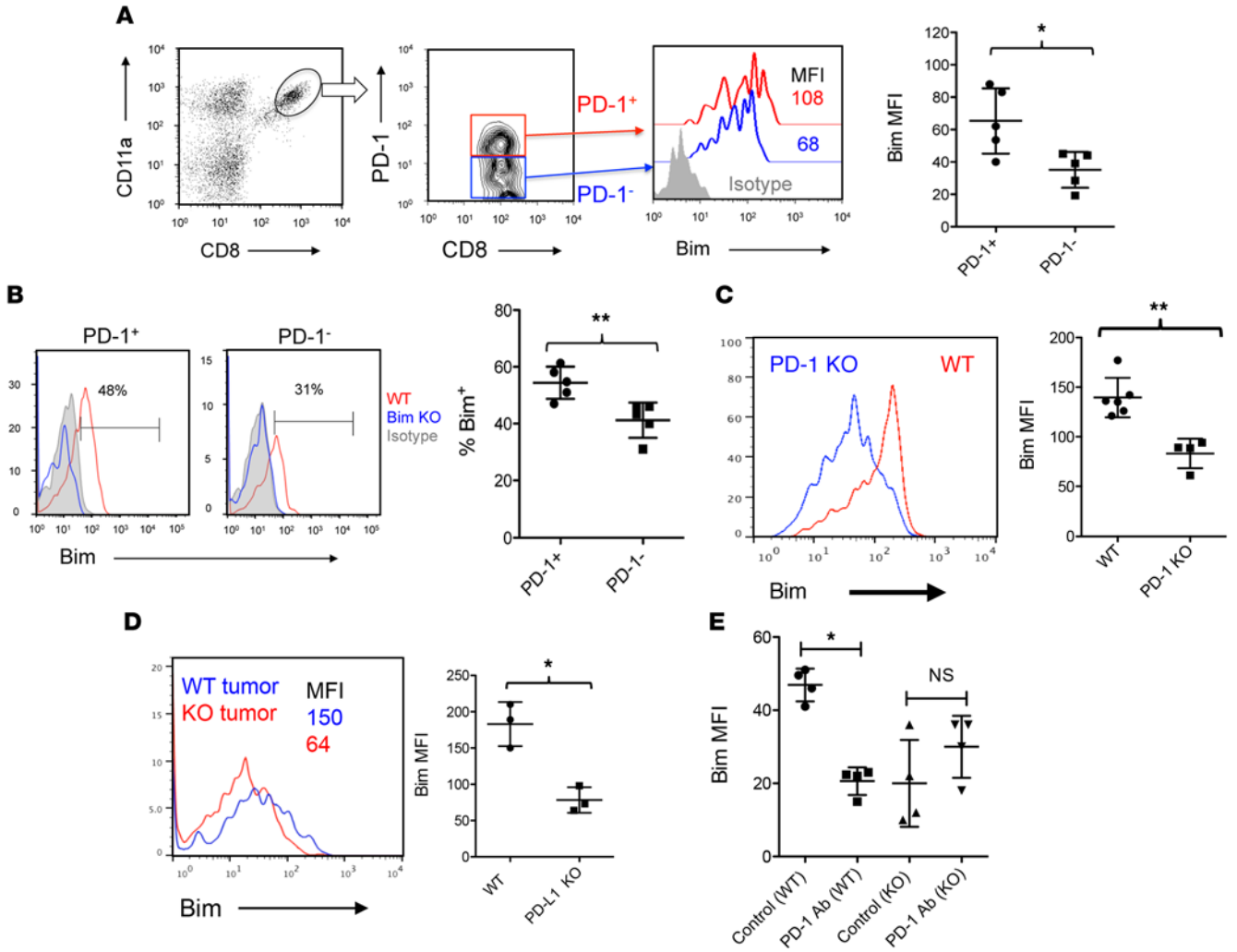

Figure 1. Bim upregulation in tumor-reactive CD8⁺ T cells is dependent on PD-1 and PD-L1 interaction. (**A**) Higher Bim expression (mean fluorescence intensity [MFI], mean ± SD) by PD-1⁺CD11a^{hi}CD8⁺ T cells isolated from B16 melanoma tumors. (**B**) Higher frequency of Bim⁺ cells among PD-1⁺CD8⁺ T cells isolated from B16 tumors of WT and Bim KO mice. (**C**) Lower Bim expression by CD8⁺ T cells isolated from B16 tumors in PD-1 KO mice than WT mice. Data in **A**–**C** were analyzed using Mann-Whitney *U* test, $*P < 0.05$, $**P < 0.01$. (**D**) Bim expression by CD8⁺ T cells isolated from WT and PD-L1 KO breast tumors. Data are from 3 to 5 mice per group and are representative of 2 independent experiments. Data were analyzed using a paired 2-tailed Student *t* test, $*P < 0.05$. (**E**) PD-1 antibody (G4) or control IgG reduced Bim levels (MFI) in PD-1⁺CD11a^{hi}CD8⁺ T cells in PD-L1 WT, but not in PD-L1 KO, tumor tissues. Data were analyzed via 1-way ANOVA with a Newman-Keuls multiple comparison test, $*P < 0.05$.

Given this variability in response and the desire to extend the long-term benefits of novel immunotherapeutic agents to more patients, there is an increased need for the development of biomarkers that can predict treatment outcomes, thereby ensuring that these expensive new treatments, which may have significant toxicities, are offered to the patients who are most likely to benefit. While tumor-associated PD-L1 expression has been proposed as a potential biomarker of response to anti–PD-1 therapy (13), durable responses have been observed in patients with PD-L1⁻ tumors, calling into question the clinical utility of PD-L1 expression alone as a predictive biomarker (5, 14, 15). Furthermore, the heterogeneity of PD-L1 expression limits its use as a predictive biomarker for PD-1 blockade (16). Therefore, since PD-1 per se is the actual therapeutic target of anti–PD-1 therapy, here we developed an individualized predictive strategy to identify patients who are most likely to respond based on biomarkers reflecting the sensitivity of their tumor-reactive PD-1⁺CD8⁺ T lymphocytes to PD-1 blockade.

In this report, we show that measurement of Bim (BCL-2-interacting mediator of cell death) as a PD-1 downstream signaling molecule can be used to predict and monitor T cell responses to anti–PD-1 therapy in melanoma patients. Since we cloned PD-L1 (17) and found that tumor-associated PD-L1 mediates tumor immune evasion (8), our group has been working on dissecting the molecular mechanisms of the

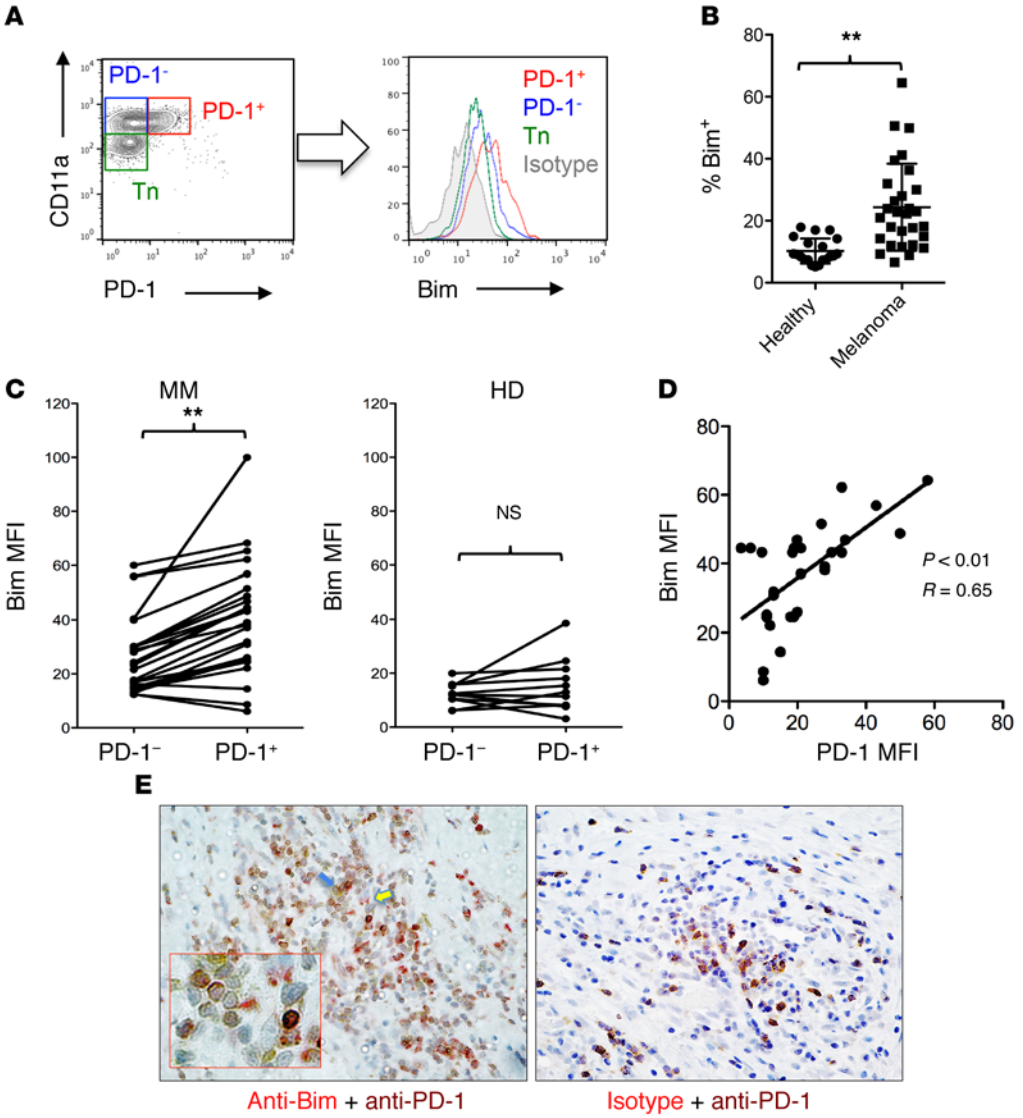

Figure 2. Bim upregulation is associated with PD-1 expression in melanoma patients. (**A**) A representative histogram shows Bim expression among subsets of CD8$^+$ T cells in the peripheral blood of metastatic melanoma (MM) patients. Tn, naive T cells. (**B**) Frequency of Bim$^+$ cells (%, mean ± SD) among PD-1$^+$CD11a^{h-i}CD8$^+$ T cells from peripheral blood of MM patients (n = 29) and healthy donors (n = 20). (**C**) Increased expression of Bim in PD-1$^+$ cells compared with that in PD-1$^-$ cells among CD11a^{hi}CD8$^+$ T cells in the peripheral blood of MM patients (n = 26) but not in healthy donors (HD, n = 20). (**D**) A positive correlation between Bim and PD-1 levels in CD11a^{hi}CD8$^+$ T cells of MM patients (n = 26). (**E**) Costaining of PD-1 and Bim in melanoma tissues. The yellow arrow indicates Bim and PD-1 double-positive tumor-infiltrating lymphocytes, blue arrow indicates PD-1 single-positive tumor-infiltrating lymphocytes. The inset is an enlarged image of cells indicated by arrows. Isotype control of Bim antibody was used with anti–PD-1 together in the right panel. Original magnification, ×400. Data in **B** and **C** were analyzed by nonparametric Mann-Whitney test, $^{**}P < 0.01$. Data in **D** were analyzed by Pearson correlation test.

PD-L1/PD-1 pathway in T cell dysfunction. Recently, we indicated that PD-L1 limits the entry of effector CD8$^+$ T cells into the memory pool by upregulating Bim, a proapoptotic molecule, in primed CD8$^+$ T cells in vivo and in vitro (18). Furthermore, we showed that PD-L1 deficiency or blockade dramatically reduced Bim levels in effector CD8$^+$ T cells and decreased T cell apoptosis (18), suggesting that Bim, a molecule known to play a crucial role in the physiologic deletion of self-reactive immune cells (19), is also an underlying mediator of PD-L1–induced T cell apoptosis (8). Based on these observations, we examined whether the interaction of PD-1 with PD-L1 is directly involved in Bim upregulation in patients with advanced cancer and whether PD-1 blockade reduces Bim levels in tumor-reactive CD8$^+$ T cells. We further translated our preclinical studies to evaluate Bim in the clinical setting as a biomarker to predict and monitor patient responses to anti–PD-1 therapy.

Results

Bim is a PD-1 downstream signaling molecule in tumor-reactive CD8$^+$ T cells. We previously demonstrated that the ligand of PD-1, PD-L1, is responsible for the upregulation of Bim in activated CD8$^+$ T cells in vivo (18). To further investigate whether PD-1 is directly involved in Bim upregulation in tumor-reactive CD8$^+$ T cells, we isolated tumor-infiltrating lymphocytes (TILs) and measured the expression of Bim in PD-1$^+$ tumor-reactive CD8$^+$ T cells identified by their high expression of CD11a (20). Both PD-1 and CD11a have been established by us and others as an identifier of tumor-reactive CD8$^+$ T cells in mouse and human melanoma systems (20, 21). As shown in Figure 1A, CD11a^{hi} tumor-reactive CD8$^+$ T cells, isolated from B16 mouse

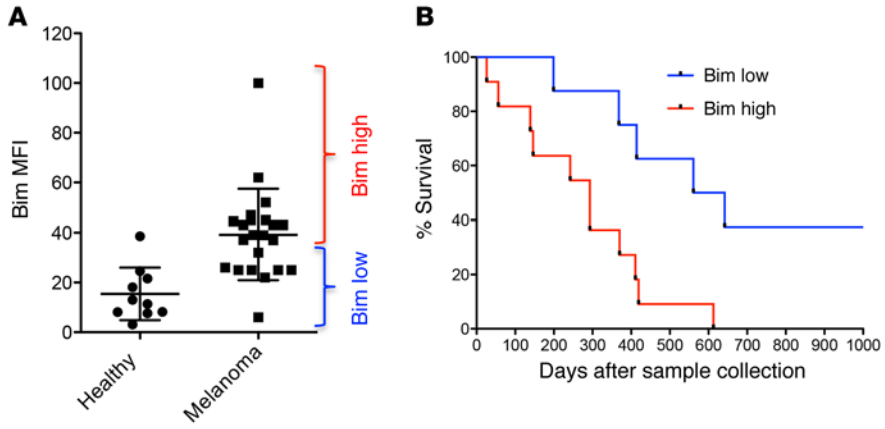

Figure 3. Bim upregulation negatively affects the survival of melanoma patients. (**A**) The optimal cut-off point of Bim levels was defined as the mean Bim levels (mean fluorescence intensity [MFI]) of healthy donors (n = 10) plus 2 SD, i.e., 15.4 + 10.5 × 2 = 36.4 (Bim MFI). This cut-off point of Bim MFI is closer to the mean Bim MFI (39.1) of melanoma patients (n = 19). (**B**) The survival curve of melanoma patients with high (n = 11) or low (n = 8) Bim levels in their tumor-reactive CD8$^+$ T cells (P = 0.006). Data in **B** were analyzed using log-rank (Mantel-Cox) test.

melanoma tumors, were divided into PD-1$^+$ and PD-1$^-$ subsets. Bim expression was higher in the PD-1$^+$ subset than in the PD-1$^-$ subset. To validate the specificity of Bim antibody, we injected B16 tumor cells into Bim KO mice and measured comparable tumor growth among WT mice and Bim KO mice (Supplemental Figure 1; supplemental material available online with this article; doi:10.1172/jci.insight.86014DS1). We then isolated TILs from tumors to examine and compare Bim levels between PD-1$^+$CD8$^+$ and PD-1$^-$CD8$^+$ T cells among WT and Bim KO mice. As shown in Figure 1B, the percentage of Bim$^+$ cells was higher in PD-1$^+$CD8$^+$ T cells than in PD-1$^-$CD8$^+$ T cells in WT mice ($P < 0.01$), according to the gating of Bim$^+$ cells based on the staining of Bim KO CD8$^+$ T cells with anti-Bim antibody or staining of WT CD8$^+$ T cells with isotype control Ig protein. Taken together, our data suggest that Bim can be specifically identified in tumor-reactive PD-1$^+$CD8$^+$ T cells.

To test whether PD-1 contributes to higher Bim expression, we injected (PD-L1$^+$) tumor cells into PD-1 KO mice and WT mice to compare Bim expression by CD8$^+$ TILs. As shown in Figure 1C, CD11a^{hi}CD8$^+$ TILs expressed lower levels of Bim in PD-1 KO mice than in WT mice ($P < 0.01$). To examine whether tumor-associated PD-L1 contributes to Bim upregulation in tumor-reactive CD8$^+$ T cells, we isolated TILs from mice implanted with WT and PD-L1 KO mouse breast tumors. PD-L1 KO mouse breast tumors were established from NeuT mice backcrossed into PD-L1 KO mice (H. Dong et al., unpublished model). In the absence of PD-L1, tumor cells induced less Bim in tumor-reactive CD11a^{hi}CD8$^+$ T cells than in WT tumors that have intact PD-L1 expression (Figure 1D). In addition, treatment with anti–PD-1 blocking antibody significantly reduced Bim levels in tumor-reactive PD-1$^+$CD11a^{hi}CD8$^+$ T cells in PD-L1 WT, but not PD-L1 KO, tumor tissues in vivo (Figure 1E). Taken together, our results suggest that Bim upregulation in tumor-reactive CD8$^+$ T cells is dependent on PD-1 and PD-L1 interaction.

Bim upregulation is correlated with PD-1 expression in melanoma patients. To examine whether Bim upregulation is a consequence of PD-1 and PD-L1 interaction in patients with cancer, we compared Bim levels (mean fluorescence intensity [MFI]) in tumor-reactive peripheral blood CD8$^+$ T cells from patients with MM (newly diagnosed) to antigen-experienced CD8$^+$ T cells from healthy donors based on their high expression of CD11a (20, 22). Tumor-reactive CD8$^+$ T cells were identified by their expression of PD-1 (23) and CD11a in the peripheral blood of melanoma patients (20). We found that the PD-1$^+$CD11a^{hi} population expressed the highest level of Bim relative to other subsets of CD8$^+$ T cells from patients with melanoma (Figure 2A). As shown in Figure 2B, the percentages of Bim$^+$ cells among PD-1$^+$CD11a^{hi}CD8$^+$ T cells were 2.4-fold higher in the peripheral blood of MM patients than in healthy donors ($P < 0.01$). To examine whether Bim upregulation is associated with PD-1 expression, we compared Bim levels between PD-1$^+$CD8$^+$ T cells and PD-1$^-$CD8$^+$ T cells in melanoma patients. As shown in Figure 2C, Bim levels were significantly higher in tumor-reactive PD-1$^+$CD8$^+$ T cells than in PD-1$^-$CD8$^+$ T cells isolated from MM patients ($P < 0.01$). In addition, Bim levels were positively correlated with PD-1 levels in tumor-reactive CD11a^{hi}CD8$^+$ T cells in this cohort of melanoma patients (Figure 2D, $P < 0.01$, R = 0. 65). In contrast, there was no difference in Bim levels between the PD-1$^+$ and PD-1$^-$ subsets in CD8$^+$ T cells of healthy donors (Figure 2C), although some antigen-experienced CD11a^{hi}CD8$^+$ T cells from healthy donors also express PD-1 (24). Interestingly, we observed that some, but not all, PD-1$^+$ TILs expressed Bim within melanoma tumor tissues (Figure 2E), implying a functional diversity of PD-1$^+$ T cells with respect to their engagement with ligands in the tumor microenvironment. The specificity of the Bim antibody used for

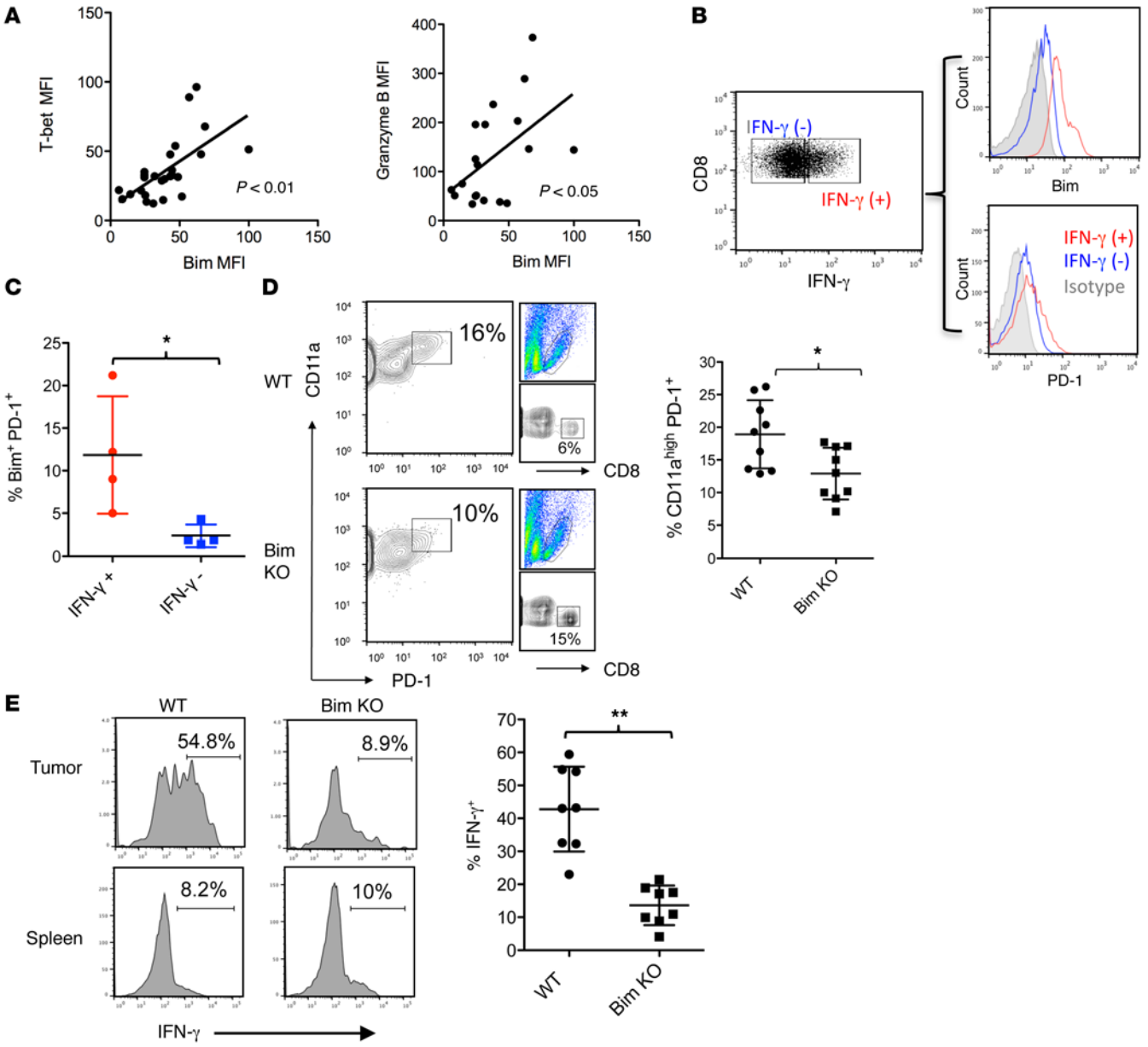

Figure 4. Bim upregulation in effector CD8⁺ T cells. (**A**) Positive correlations between Bim and granzyme B (n = 19) or T-bet (n = 26) levels in CD11a^{hi}CD8^{+} T cells of melanoma patients. (**B**) High Bim and PD-1 expression in IFN-γ–producing CD8^{+} T cells stimulated with PMA and ionomycin. (**C**) Tumor antigen-specific effector (IFN-γ^{+}) CD8^{+} T cells have higher expression of Bim and PD-1 than noneffector (IFN-γ^{-}) cells. Data in **A** and **B** were analyzed by Pearson correlation test. Data in **C** are from 4 MM patients per group and are representative of 2 independent experiments, $^{*}P < 0.05$ (2-tailed unpaired t test). (**D**) Frequency of PD-1^{+}CD11a^{hi} cells among CD8^{+} T cells within B16 tumor tissues of WT and Bim KO mice (n = 9). The right-sided graphs show percentages of CD8^{+} T cells in tumor-infiltrating lymphocytes. (**E**) Frequency of IFN-γ–producing CD8^{+} T cells from tumor tissues of WT and Bim KO mice (n = 8). The background production of IFN-γ was shown in spleens of naive mice. Data in **D** and **E** were analyzed by Mann-Whitney U test, $^{*}P < 0.05$, $^{**}P < 0.01$.

tissue staining was validated by preblocking with Bim protein (Supplemental Figure 2). Consistent with our preclinical work (18), these clinical studies indicate that Bim upregulation is dependent on PD-1 expression by tumor-reactive CD8^{+} T cells in patients with MM.

Bim upregulation has a negative impact on survival of patients with MM. Given the proapoptotic role of Bim in activated CD8^{+} T cells (25, 26) as a consequence of PD-1 interaction with PD-L1 expressed by tumor cells, Bim upregulation may exert a negative impact on the clinical outcome of cancer patients. To that end, we compared overall survival in a cohort of patients with newly diagnosed unresectable MM who did not receive anti–PD-1 therapy and in whom we measured Bim expression in PD-1^{+}CD8^{+} T cells. Since Bim expression by PD-1^{+}CD8^{+} T cells was identified in both healthy donors and MM patients (Figure 2C),

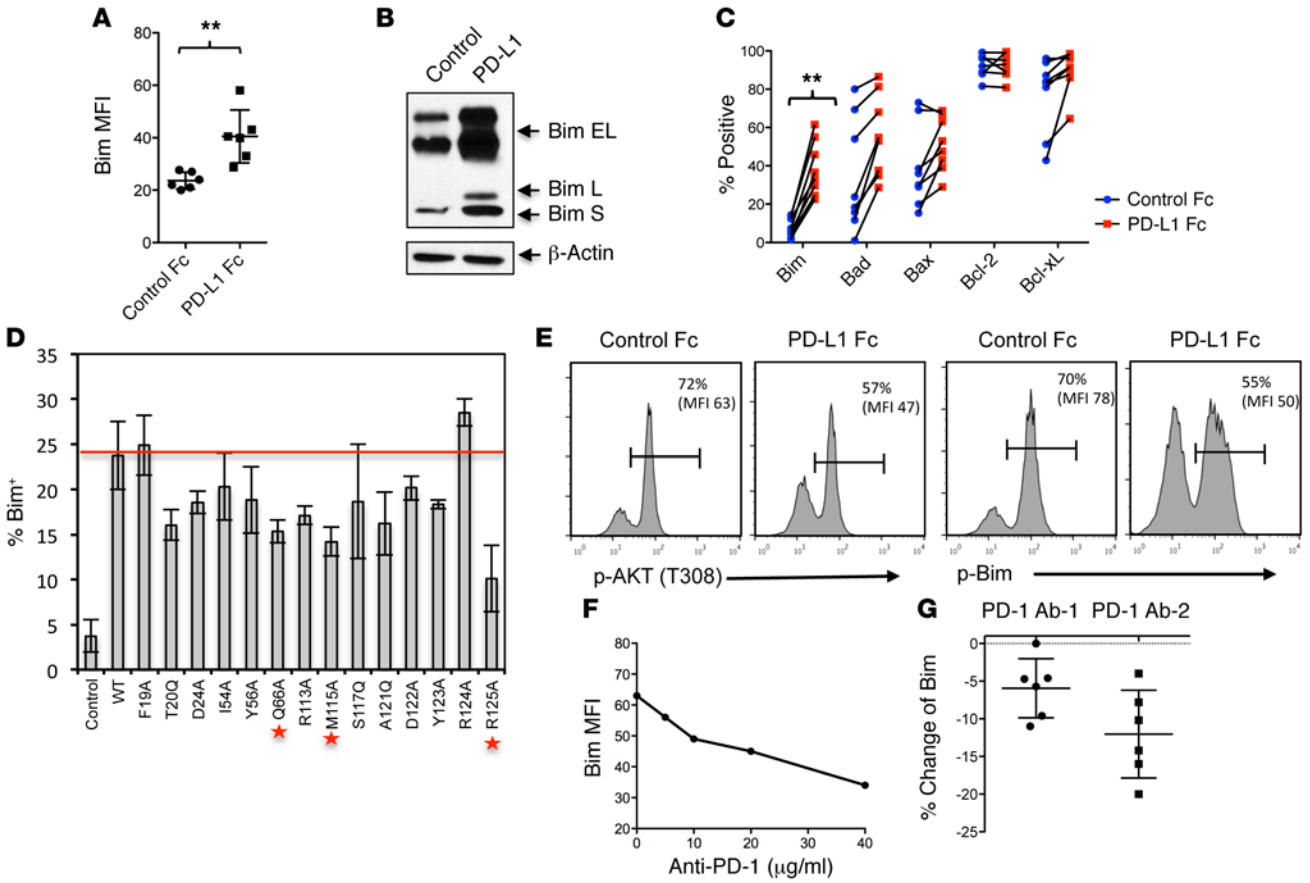

Figure 5. PD-1 blockade decreases Bim expression induced by PD-L1 in human CD8⁺ T cells. (**A**) PD-L1 fusion protein induced Bim upregulation in preactivated human CD8⁺ T cells analyzed in vitro by flow cytometry. (**B**) Western blotting shows increased expression of Bim isoforms (EL, extra long; L, long; S, short) in CD8⁺ T cells stimulated with PD-L1 protein compared with control protein. The full unedited gel is shown in Supplemental Figure 4. (**C**) Frequencies of expression of some Bcl-2 family proteins in primary human CD8⁺ T cells stimulated with PD-L1 or control fusion proteins. Lines indicate each individual donor (n = 8). Data in **A** and **C** were analyzed using a Mann-Whitney U test, $^{**}P < 0.01$. (**D**) Percentages (mean ± SD of 3 donors) of Bim⁺ cells in CD8⁺ T cells stimulated with PD-L1 mutants. The red line indicates the percentage of the Bim⁺ population induced by WT PD-L1. Stars indicate critical sites in human PD-L1 for binding to PD-1. (**E**) PD-L1–induced downregulation of AKT activation and phosphorylation of Bim. (**F**) Dose-dependent blocking effects of anti–PD-1 antibody (MIH4) on Bim levels (mean fluorescence intensity [MFI]) induced by PD-L1. (**G**) Two versions of humanized anti–PD-1 antibodies (Ab-1 and Ab-2) decreased Bim expression induced by PD-L1 in human CD8⁺ T cells. Data are from 6 donors per group and are representative of 2 independent experiments.

we defined high Bim levels as above the mean level of Bim (MFI) plus 2 SD (i.e., 36.4) of healthy donors (Figure 3A); this Bim level was also closer to the mean Bim MFI (39.1) of melanoma patients. As shown in Figure 3B, melanoma patients with higher Bim expression (>36.4 MFI, n = 11), had significantly shorter survival compared with patients with lower Bim (≤36.4 MFI, n = 8; 9.7 vs. 20 months, $P < 0.05$). Since we measured Bim levels before any treatment, we postulated that Bim upregulation in PD-1⁺CD8⁺ T cells negatively affects survival in advanced melanoma. These data also provided a rationale to test whether patients with different levels of Bim expression would respond differently to anti–PD-1 therapy.

Bim identifies PD-1⁺ tumor-reactive CD8⁺ T cells with effector function. Bim is a proapoptotic molecule that contributes to the deletion of most active effector CD8⁺ T cells at the contraction phase of a T cell response (19, 27, 28). To examine whether Bim is a regulator of apoptosis in tumor-reactive effector CD8⁺ T cells in patients with melanoma, we examined the association of Bim with effector CD8⁺ T cell markers, T-bet, a transcription factor of effector CD8⁺ T cells (29), and granzyme B, a functional molecule of effector CD8⁺ T cells (30). Interestingly, Bim expression had a significantly positive association with T-bet and granzyme B among circulating PD-1⁺ tumor-reactive CD8⁺ T cells in melanoma patients (Figure 4A). These results suggest that Bim upregulation is a unique feature of PD-1⁺CD8⁺ T cells with effector function. Next, we examined whether CD8⁺ T cells at their effector phase, i.e., upon activation or antigen stimulation, express higher Bim or PD-1 than in the resting phase. First, we stimulated CD8⁺ T cells with PMA and ionomy-

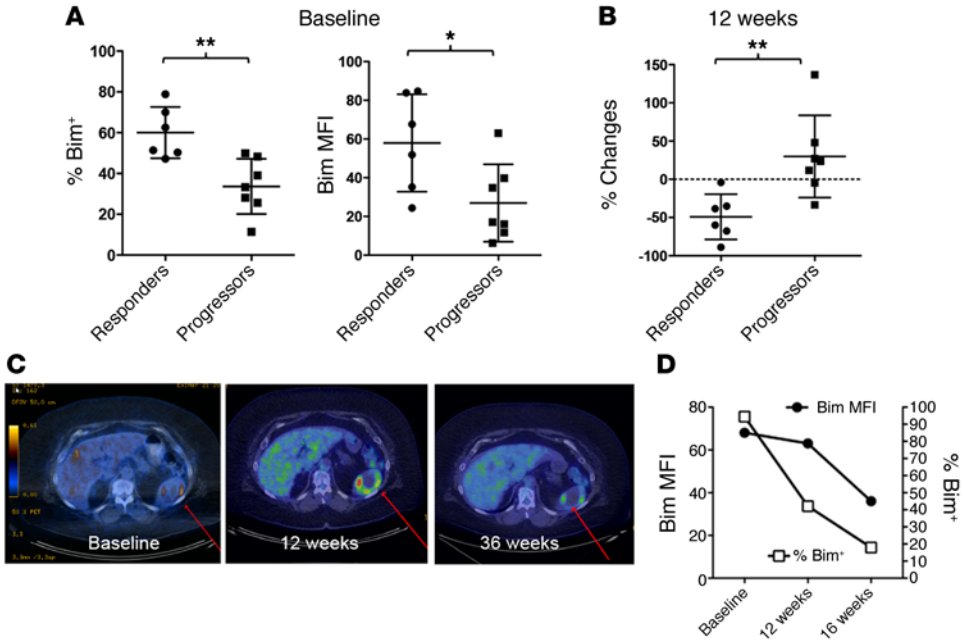

Figure 6. Changes of Bim levels predict responses to anti–PD-1 therapy in melanoma patients. (**A**) Bim levels (frequency [%] and mean fluorescence intensity [MFI]) among PD-1$^+$CD11a^{hi}CD8$^+$ T cells at baseline in melanoma patients with progressive diseases (n = 7) and responders (n = 6). (**B**) Percentages of changes in the frequency of Bim$^+$ cells among PD-1$^+$CD11a^{hi}CD8$^+$ T cells at 12 weeks after anti–PD-1 (pembrolizumab) therapy of the same cohort of patients as in **B**. Data in **A** and **B** were analyzed by nonparametric Mann-Whitney test, $^*P < 0.05$, $^{**}P < 0.01$; error bars, median with interquartile ranges. (**C**) Imaging of metastatic melanoma (red arrows) in one patient with pseudoprogression at 12 weeks after anti–PD-1 therapy. (**D**) The changes of Bim levels (% and MFI) among circulating PD-1$^+$CD11a^{hi}CD8$^+$ T cells of this patient at baseline and 12 and 16 weeks after PD-1 therapy.

cin to initiate T cell activation. Among IFN-γ–producing CD8$^+$ T cells, we found higher Bim and PD-1 expression than in non-IFN-γ–producing cells (Figure 4B), suggesting that activated T cells with effector function indeed express higher levels of Bim and PD-1. Besides PMA and ionomycin, which induce antigen-independent T cell activation, we measured the expression of Bim and PD-1 in effector CD8$^+$ T cells that were stimulated by tumor antigens. CD8$^+$ T cells isolated from melanoma patients were stimulated with melanoma antigens (MART-1 and gp100). Tumor antigen-specific effector CD8$^+$ T cells were identified by their production of IFN-γ. As shown in Figure 4C, Bim and PD-1 expression was dominant in the IFN-γ–producing population compared with the non-IFN-γ–producing population.

To confirm the role of Bim in T cell activation and effector function, we examined and compared the generation and function of tumor-reactive CD8$^+$ T cells among WT and Bim KO mice. A lower frequency of tumor-reactive (PD-1$^+$CD11a^{hi}) CD8$^+$ T cells was generated in tumors of Bim KO mice than in WT mice, although the total percentage of CD8$^+$ T cells increased in tumors of Bim KO mice (Figure 4D). Additionally, tumor-reactive CD8$^+$ T cells in Bim KO mice produced less IFN-γ than in WT mice (Figure 4E). This defect of IFN-γ production in Bim KO mice seems to be tumor-related, because both WT and Bim KO CD8$^+$ T cells isolated from spleens of naive mice produced comparable baseline levels of IFN-γ upon ex vivo stimulation (Figure 4E). Taken together, our results suggest that Bim is required for CD8$^+$ T cell activation in order to generate effector cells, and Bim upregulation could be a sign for activated CD8$^+$ T cells with effector function.

PD-1 blockade decreases Bim expression induced by PD-L1 in human CD8$^+$ T cells. Anti–PD-1 therapy is aimed at blocking the interaction of PD-1 and its ligands in order to restore T cell function or rescue T cells from death. Since Bim upregulation is a consequence of PD-1 and PD-L1 interaction, this suggests that anti–PD-1 blocking antibody may be able to reduce PD-L1–induced Bim upregulation in T cells. We previously reported that PD-L1 stimulation enhances apoptosis of T cells activated by TCR stimulation (18). Using a similar approach, we established an in vitro system to induce Bim upregulation by PD-L1 in human activated CD8$^+$ T cells. PD-L1 dramatically increased Bim levels in preactivated CD8$^+$ T cells, as analyzed by flow cytometry (Figure 5A). In addition, PD-L1–induced upregulation of Bim was confirmed by Western blotting (Figure 5B). To explore whether other proapoptotic or antiapoptotic proteins change along with Bim in human T cells upon PD-L1 stimulation, we measured the expression of each

proapoptotic (Bim, Bad, and Bax) and antiapoptotic (Bcl-2 and Bcl-xL) molecule in human primary $CD8^+$ T cells stimulated with or without PD-L1 fusion protein in vitro. As shown in Figure 5C, although PD-L1 stimulation individually increased the expression of proapoptotic (Bim, Bad, and Bax) and antiapoptotic molecules (Bcl-xL) compared with the control protein, only Bim changes reached statistical significance ($P < 0.05$). In contrast, Bcl-2 was expressed by most of $CD8^+$ T cells and did not change upon PD-L1 stimulation. To further confirm that Bim overexpression in human primary $CD8^+$ T cells by PD-L1 protein is dependent on the interaction with PD-1, we screened a number of PD-L1 mutants for their ability to stimulate Bim upregulation in human $CD8^+$ T cells. We found that PD-L1 mutants at Q66A, M115A, and R125A markedly disrupted the ability of PD-L1 to induce Bim upregulation (Figure 5D). Since these 3 amino acids reside at sites that are critical for PD-L1 binding to PD-1 (31), our data confirmed that Bim upregulation induced by PD-L1 is via PD-1/PD-L1 interaction. We previously reported that PD-L1 regulates Bim expression through suppression of AKT activation in mouse $CD8^+$ T cells (18). To examine whether a similar mechanism applies to human $CD8^+$ T cells, we measured phosphorylated AKT in human $CD8^+$ T cells upon PD-L1 stimulation. As shown in Figure 5E, PD-L1 stimulation reduced phosphorylated AKT levels compared with control protein stimulation, suggesting a mechanism similar to PD-L1–mediated AKT suppression, as in mouse $CD8^+$ T cells. Since AKT activation enhances Bim phosphorylation leading to Bim degradation (32), we measured the levels of phosphorylated Bim after PD-L1 stimulation. Interestingly, PD-L1 decreased phosphorylated Bim in human activated $CD8^+$ T cells (Figure 5E). Our results suggest that PD-L1–induced Bim upregulation may be a result of decreased degradation of Bim via suppression of AKT activation by PD-L1 and PD-1 interaction in T cells.

To test whether Bim upregulation induced by PD-L1 could be blocked by anti–PD-1 antibody, we screened several commercial available mouse anti-human PD-1 antibodies for their blocking effects and found one anti–PD-1 antibody clone (MIH4) that markedly blocked Bim upregulation induced by PD-L1 in a dose-dependent fashion (Figure 5F). Additionally, we tested the blocking effects of two humanized monoclonal antibodies against human PD-1 currently being used in clinical practice in patients with MM and lung cancer. Both antibodies demonstrated blocking effects in Bim upregulation induced by PD-L1 in human activated $CD8^+$ T cells (Figure 5G) at the same dose (10 μg/ml). Taken together, our results indicate that PD-1 interaction with PD-L1 leads to upregulation of Bim in human activated $CD8^+$ T cells and PD-1 blockade reduces Bim expression induced by PD-L1.

Bim levels identify responders to anti–PD-1 therapy in MM. Based on our preclinical evidence that Bim levels reflect the degree of PD-1 interaction with PD-L1 in tumor-reactive $CD8^+$ T cells, we next tested whether Bim could be used as a noninvasive monitoring or predictive biomarker to evaluate T cell responses in patients with cancer undergoing treatment with an anti–PD-1 monoclonal antibody. Among the 38 patients with melanoma who received anti–PD-1 (pembrolizumab) therapy on an expanded access program (see the Methods section), we identified 13 evaluable patients who had an unequivocal radiographic objective tumor response (6 patients) or progression (7 patients) at the first tumor assessment at 12 weeks and for whom we had baseline and 12-week peripheral blood samples available (Supplemental Table 1). As high Bim levels would predictably lead to increased T cell apoptosis, we initially hypothesized that patients with high Bim expression would be resistant to PD-1 blockade. On the contrary, we found that patients who experienced clinical benefit (either a complete response [CR] or partial response [PR]) after 4 cycles of anti–PD-1 therapy had a higher frequency of $Bim^+PD\text{-}1^+CD8^+$ T cells in the peripheral blood and higher Bim MFI at baseline compared with patients with radiographic progression (Figure 6A and Supplemental Table 2). In addition, the frequencies of $Bim^+PD\text{-}1^+CD8^+$ T cells decreased significantly after the first 3 months of treatment in all responders compared with progressors (Figure 6B and Supplemental Table 2), including two patients who were found to have pseudoprogression at 12 weeks (progression on PET scan without CT correlate in one case and with negative biopsy in another case). In one patient described below, we measured a dramatic decline in the percentage of Bim^+CD8^+ T cells at 12 weeks (after 4 doses of anti–PD-1 therapy), while the PET scan showed progressive disease in the spleen (red arrow, Figure 6, C and D). Before the PET scan eventually confirmed improvement in the fluorodeoxyglucose-avid lesions at the same site (red arrow, Figure 6C) at 36 weeks, we identified further decline in Bim levels (both in percentages and MFI) in circulating tumor-reactive $CD8^+$ T cells at 16 weeks after initial PD-1 therapy (Figure 6D). Our results suggest that measurement of Bim levels could be used to monitor objective responses to anti–PD-1 therapy, especially in patients who might have radiographic pseudoprogression of disease.

In contrast to patients with pseudoprogression, 5 of 7 patients who experienced radiographic disease progression had increased Bim levels at 12 weeks (range, 12%–137%) and discontinued therapy either immediately or at the next tumor assessment at 24 weeks. Two patients with radiographic disease progression at week 12 were found to have a decrease in Bim levels by 5% and 33%, respectively. The patient with a minimal change in Bim levels (–5%) ultimately experienced unequivocal tumor progression at 24 weeks and discontinued therapy. The patient with a more substantial decrease in Bim (–33%) was found to have isolated central nervous system progression at 12 weeks, with stable extracranial disease, and was continued on anti–PD-1 therapy for more than 12 months after completion of whole-brain radiation therapy. Taken together, our results suggest that measuring Bim levels in tumor-reactive $CD8^+$ T cells could be used to a priori select patients who may derive clinical benefit from anti–PD-1 therapy and monitor responses during treatment.

Discussion

Here, we report that Bim is a downstream signaling molecule of PD-1, which reflects the degree of PD-1 interaction with its ligand PD-L1 in tumor-reactive effector $CD8^+$ T cells. While the mechanisms of T cell apoptosis induced by tumor-associated PD-L1 are not clearly identified, our results suggest that upregulation of Bim as a result of PD-1/PD-L1 interaction may contribute to the deletion of tumor-reactive $PD\text{-}1^+CD8^+$ T cells. On the other hand, we demonstrate that Bim could also be used to identify effector $CD8^+$ T cells that are under the regulation of the PD-1 pathway. We show that the increased frequencies (percentages) of $Bim^+PD\text{-}1^+CD8^+$ T cells in a subset of patients with MM reflect the presence of an increased number of effector $CD8^+$ T cells responsive to PD-1 blockade and may ultimately predict response to therapy. In the current study, we found that patients who experienced clinical benefit (patients with CR, PR, or stable disease) after 4 cycles of anti–PD-1 therapy had a higher frequency of Bim^+ cells among $PD\text{-}1^+CD11a^{hi}CD8^+$ T lymphocytes in the peripheral blood at baseline compared with patients with radiographic progression. We hypothesize that this is likely due to an abundant PD-1 interaction with its tumor-associated ligand PD-L1. Indeed, our findings are in agreement with previous reports of worse survival (33), yet higher objective responses to anti–PD-1 therapy, in patients with $PD\text{-}L1^+$ tumors (9, 34), with higher PD-L1 expression levels capturing the most PD-1–responsive population (35). The question remains of whether there is a threshold of Bim upregulation in individual T cells that would distinguish PD-1–expressing T cells, which have become committed to cell death, from those that have yet to fully engage their apoptotic machinery and could theoretically be reversed to be functionally engaged.

While the proapoptotic activity of Bim during lymphocyte development and termination of the immune response is well described (28), our studies suggest that Bim could also have a bifunctional role in regulating both T cell death and activation. We found a positive association between expression of Bim and effector-related molecules (T-bet and granzyme B) in circulating tumor-reactive $PD\text{-}1^+CD8^+$ T cells in melanoma patients (Figure 4A) and showed that Bim is upregulated in the effector $CD8^+$ T cells upon tumor antigen stimulation ex vivo (Figure 4B). In addition, we indicate that Bim is required for generation of functional tumor-reactive effector $CD8^+$ T cells in vivo (Figure 4, D and E). These results could explain why circulating T cells with high levels of Bim, although they are prone to apoptosis, are still detectable in the peripheral blood of cancer patients. Indeed, the increased levels of Bim in $PD\text{-}1^+CD8^+$ T cells from patients with MM may reflect a recent encounter with the relevant tumor antigens. Our results are in agreement with reports of reduced effector function in Bim-deficient T cells in response to self-antigen or allo-antigen stimulation (36, 37). In addition, recent studies suggest that effector T cell–derived IFN-γ is a primary inducer of PD-L1 expression in the tumor microenvironment (38). However, the mechanism by which Bim participates in T cell activation is not completely understood and warrants further investigation. It is possible that Bim could either compete with Bcl-2 or Bcl-xL in forming a complex with the inositol triphosphate receptor on the endoplasmic reticulum to modulate Ca^{+2} release (36) or contribute to phosphorylation of PLCγ, a key step in TCR signaling pathway for T cell activation (37).

Moreover, it is still unclear how effector T cells with high levels of Bim balance T cell activation or apoptosis, and this process could be dependent on the immunological context. Our results and those of others collectively suggest that Bim upregulation is a result of TCR stimulation in effector cells (refs. 39, 40, and Figure 4B). A potential mechanism for effector lymphocytes to tolerate high levels of Bim is to increase Bcl-2 (40). Actually, high levels of Bim and Bcl-2 have been identified in a subset of murine effector $CD8^+$ T cells with a long life span following infection, and Bcl-2 depletion leads to a significant loss of this population (40). However, Bim upregulation by TCR stimulation alone may not be able to exceed the threshold

needed to initiate apoptosis, at least in the circulating blood. Once tumor-reactive T cells are exposed to their antigen at the tumor site, they interact with PD-L1 abundantly expressed by the tumor cells, and this process could further increase Bim and tip the balance in favor of T cell apoptosis (8). This hypothesis is in agreement with our findings regarding the ability of PD-L1 to increase Bim but not Bcl-2 or Bcl-xL (Figure 5C). Therefore, circulating tumor-reactive PD1$^+$CD8$^+$ T cells with high levels of Bim are virtual effector cells en route to tumors; they are not dying because they have not yet engaged PD-L1 in the systemic circulation, but they will eventually undergo apoptosis if they encounter PD-L1 expressed at the tumor sites.

Interestingly, a potential prognostic/predictive role of Bim in malignant cells, but not in T cells, has been proposed in some solid cancers, such as EGFR mutant lung cancer. Recent studies have shown that, in cells dependent upon mutant EGFR signaling for survival, EGFR kinase inhibition reduces Bim levels through Bim dephosphorylation. In these studies, the enhanced proapoptotic activity of Bim seems to be required for tyrosine kinase inhibitor–induced cell death. Among patients with EGFR mutant non–small-cell lung cancer included in the randomized phase III EURTAC trial (41) comparing erlotinib with chemotherapy, high Bim expression in the tumor was identified as a marker of longer progression free survival and overall survival (42, 43).

Similarly, our results provide a strong rationale for the use of PD-1 blockade in patients with high levels of Bim because of their high risk of death and the presence of an increased target CD8$^+$ T cell population that contains potentially reversible tumor-reactive (PD-1$^+$CD11a^{hi}) CD8$^+$ T cells. Since high Bim levels are associated with tumor-reactive CD8$^+$ T cells with effector function, our findings also imply that tumor-reactive CD8$^+$ T cells at their effector phase may represent the T cell population that is most sensitive to PD-1 regulation. High Bim expression may identify a population of effector cells in which PD-1 has engaged PD-L1. Thus, the high frequency of Bim$^+$CD8$^+$ T cells in responders to anti–PD-1 therapy (Figure 6A) not only suggests that responders may harbor more tumor-reactive effector CD8$^+$ T cells than nonresponders, but also that these cells may be more sensitive to the regulation of PD-1. In these patients, the higher frequency of Bim$^+$CD8$^+$ T cells suggests that they have an increased number of effector cells that have been recently primed by relevant tumor antigens and can be rescued by PD-1 blockade to augment the antitumor immune response. On the other hand, the lower frequency of Bim$^+$CD8$^+$ T cells in nonresponders (Figure 6A) suggests either the availability of fewer effector cells or decreased tumor antigen stimulation; in either case, PD-1 blockade was not able to make a significant impact in this clinical context. Interestingly, after 12 weeks of treatment, the frequency of Bim$^+$CD8$^+$ T cells decreased dramatically in the responders (Figure 6B), suggesting less stimulation with tumor antigens or with tumor-associated PD-L1 likely due to tumor regression. Interestingly, patients who experienced pseudoprogression at the time of the first tumor assessment had a decreased frequency of peripheral blood Bim$^+$CD8$^+$ T cells and decreased Bim MFI at 12 weeks compared with baseline (Figure 6, C and D), suggesting a consistency of peripheral T cell Bim levels and an ultimate tumor response to anti–PD-1 therapy. We also noted that more PD-1$^+$CD11a^{hi}CD8$^+$ T cells were retained in the peripheral blood after 4 cycles of therapy in the group of patients who experienced objective responses (patients with CR or PR) compared with patients with no clinical benefit, although the change was not statistically significant (Supplemental Table 2).

Although PD-1$^+$ tumor-reactive CD8$^+$ T lymphocytes were the main effector cells expressing high levels of Bim in the tumor microenvironment, we also identified high Bim expression in NK cells but not in CD4 T cells (Supplemental Figure 3). Since most of NK cells isolated from tumor tissues, but only a small percentage of NK cells isolated from the spleen, expressed Bim, our results imply that NK cells may also be subject to the regulation mediated by the PD-L1/PD-1 pathway within the tumor immune milieu. The clinical implication of Bim expressed by tumor-associated NK cells is interesting; it suggests that the innate immune response to tumors could be a new target for immune checkpoint therapies, which warrants further investigation. Indeed, understanding how to precisely manipulate PD-1 and its receptors may provide unique opportunities for designing novel combinatorial therapies.

Limitations of our study include the relatively small cohort of patients and the fact that only one anti–PD-1 antibody (pembrolizumab) was used clinically. Therefore, we are currently prospectively evaluating larger cohorts to determine the threshold for Bim upregulation in individual T cells that would distinguish PD-1$^+$CD11a^{hi}CD8$^+$ T cells that have become committed to cell death from those that have yet to fully execute their apoptotic machinery. Similarly, future work is focusing on defining to what degree a reduction of Bim levels could theoretically be achieved by PD-1 blockade. Since our study mainly focused on the changes of Bim levels in circulating PD-1$^+$CD11a^{hi}CD8$^+$ T cells, what degree the changes in the peripheral

blood correlate with those in the tumor tissue is still an open question. In addition, future studies are warranted to evaluate whether Bim could be used in the monitoring of other tumor types with respect to their responses to anti–PD-1 therapy.

In conclusion, our findings indicate that measurement of Bim levels (frequency and MFI) in tumor-reactive PD-1$^+$CD11a^{hi}CD8$^+$ T cells in the peripheral blood of patients with MM may be a less invasive and more sensitive strategy to monitor or possibly predict responses to anti–PD-1 therapy. Our results are clinically significant because the discovery of biomarkers of sensitivity is vital for informing clinical decision-making, not only in selecting those patients with MM (and possibly other malignancies) who are most likely to benefit from the immunotherapy, but in identifying those patients with late therapeutic responses, thereby exposing fewer patients to inadequate treatments and their associated toxicities and costs. In addition, a great advantage of our approach lies in the ease of serial peripheral blood testing as compared with repeated invasive tissue biopsies.

Methods

Detection of human tumor-reactive CD8$^+$ T cells. Peripheral blood mononuclear cell (PBMC) samples were collected from patients with melanoma. Antibodies for CD8, CD11a (HI111), PD-1 (EH12.2H7) were purchased from BioLegend and IFN-γ (4S.B3) was purchased from eBioscience. The tumor antigen specificity of CD11a^{hi}PD-1$^+$CD8$^+$ T cells was confirmed by staining with HLA-A2/MART-1 tetramer. The function of human tumor-reactive CD8$^+$ T cells was measured by intracellular staining for IFN-γ. Briefly, lymphocytes were incubated with MART-1 and gp100 (Mayo Clinic Peptide Core) at 1 μg/ml of each or PMA (50 ng/ml)/ionomycin (500 ng/ml) for 5 hours. After incubation, cells were stained for surface markers followed by intracellular staining for IFN-γ. To enrich tumor antigen-specific CD8$^+$ T cells, PBMCs of melanoma patients were incubated with antigen peptides for 1 week in complete RPMI medium containing human IL-2 (10 U/ml, Proleukin, Mayo Pharmacy) before functional analysis.

Measurement of intracellular proteins in tumor-reactive CD8$^+$ T cells. Following cell surface staining for CD11a and PD-1, CD8$^+$ T cells were incubated with purified anti-mouse CD16/32 antibody for blocking nonspecific binding of immunoglobulin to Fc receptors. To detect intracellular Bim, granzyme B, or T-bet, cells were incubated with Fixation Buffer (BioLegend), followed by permeabilization using permeabilization wash buffer (Biolegend). Anti-Bim rabbit monoclonal antibody (clone C34C5; catalog 2933), anti-Bax (D2E11, 5023), anti-Bad (D24A9, 9239), anti–Bcl-2 (50E3, 2870), anti–Bcl-xL (54H6, 2764), and appropriate isotype control (rabbit [DA1E] monoclonal Ab IgG XP) were purchased from Cell Signaling and were added into cells and incubated for an hour. After staining, cells were washed 3 times with washing buffer before analysis. FITC- or PE-conjugated secondary antibody to rabbit IgG was used for flow cytometry assay. At least 100,000 viable cells were live gated on a FACSCailbur of FACSCanto instrument (BD Biosciences). Flow cytometry analysis was performed using FlowJo software (Tree Star). Bim expression was presented by frequency of Bim$^+$ cells among tumor-reactive CD8$^+$ T cells or Bim levels (MFI) in tumor-reactive CD8$^+$ T cells.

Costaining of PD-1 and Bim in human tumor tissues. Paraffin-embedded tissue sections were cut into 5-μm sections and deparaffinized. After antigen retrieval, sections were washed in running distilled H_2O and wash buffer. Sections were blocked for 5 minutes with Endogenous Peroxidase Block (Dako S2001) and washed and blocked for 5 minutes in Background Sniper (Biocare Medical BS966L). Slides were incubated overnight at 4°C in rabbit anti-human Bim (Cell Signaling 2933s, clone C34C5) monoclonal antibody diluted 1:100 in DaVinci Green Antibody Diluent (BioCare Medical PD900L). Sections were washed and incubated for 15 minutes each in rabbit probe and rabbit polymer AP (Mach 3 Rabbit AP Polymer Detection Kit, BioCare Medical M34533L). Sections were visualized using Warp Red Chromogen (BioCare Medical WR806H) for 5 minutes. Subsequently, sections were incubated for 5 minutes in 80°C Citrate Buffer (Dako S2369), pH 6, rinsed in wash buffer, and incubated in Background Sniper for 5 minutes. Mouse monoclonal anti-human PD-1 (Abcam ab52587, clone NAT105) was applied to sections at 1:400 dilution and incubated for 1 hour at room temperature. Sections were washed and incubated for 10 minutes each in mouse probe and mouse polymer HRP (Mach 3 Mouse HRP Polymer Detection kit, Biocare Medical M3M530L) and visualized for 1 minute in DAB (Biocare Medical BDB2004L). Sections were counterstained with hematoxylin and coverglass mounted with Permount.

Patient population and study design. Patients with histologically confirmed unresectable MM who were eligible to start therapy with the anti–PD-1 monoclonal antibody pembrolizumab under an expanded

access program (MK-3475-030, NCT02083484) were offered participation in an IRB-approved biomarker substudy at our institution (IRB 430-00). Eligibility criteria for enrollment in the expanded access program included progression on prior ipilimumab therapy and on BRAF inhibition therapy if BRAF mutant, age over 18 years, Eastern Cooperative Oncology Group performance status of 0 to 2, adequate organ function, and life expectancy ≥3 months. Patients with previously treated brain metastases had to be clinically stable. Major exclusion criteria were active infections or autoimmune diseases or receiving systemic immune suppressive therapy or live-virus vaccines. Patients were treated with pembrolizumab 2 mg/kg i.v. over 30 minutes every 3 weeks. Peripheral blood was collected at baseline, prior to initiation of anti–PD-1 therapy, and at the time of first radiographic tumor assessment at 12 weeks for all patients. Subsequently, every effort was made to further collect peripheral blood samples at each subsequent radiographic tumor evaluation for patients continuing on anti–PD-1 therapy. Radiographic tumor assessment was done per clinical practice with the choice of imaging left at the discretion of the treating physician.

Bim upregulation in human primary T cells. Human preactivated $CD8^+$ T cells were purified from PBMCs that had been incubated with PHA-L (Sigma-Aldrich, 5 μg/ml per 10^6 cells) for 48 hours. To induce Bim upregulation, preactivated $CD8^+$ T cells were incubated with plate-bound PD-L1 (B7-H1) fusion protein (R&D Systems) or control fusion protein in the presence of anti-CD3 antibody. Human PD-L1 mutant proteins were purchased from BPS Bioscience. After 24 hours of stimulation with PD-L1, cells were harvested and analyzed for intracellular Bim expression using flow cytometry or Western blotting assay. To block PD-1/PD-L1 interaction-induced Bim upregulation, preactivated $CD8^+$ T cells were incubated with 10 μg/ml of mouse anti-human PD-1 antibody (clone MIH4, eBioscience, special order for functional grade-purified version) or humanized antibody to PD-1 (Keytruda or Opdivo, Mayo Clinic Pharmacy) for 20 minutes before culture with PD-L1 fusion protein.

Mice, cell lines, and reagents. Female C57BL/6 and BALB/c mice were purchased from Taconic Farms and were used at an age of 12 weeks. PD-1 KO C57BL/6 mice were provided by L. Chen (Yale University, New Haven, Connecticut, USA) with the permission of T. Honjo (Kyoto University, Kyoto, Japan). The *Bcl2l11*$^{-/-}$ (Bim KO) mice on a C57BL/6 background were purchased from Jackson Laboratory. Mice were maintained under pathogen-free conditions and used at 8 to 12 weeks of age. PD-L1 WT or KO tumor cells were isolated from WT breast cancer NeuT mice provided by L. Pease (Mayo Clinic, Rochester, Minnesota, USA) or from PD-L1 KO NeuT mice (Mayo Clinic, Rochester, Minnesota, USA). B16 or B16-OVA murine melanoma cells were provided by R. Vile (Mayo Clinic, Rochester, Minnesota, USA). All cell lines were free of *Mycoplasma* contamination (Mycoplasma Detection kit; Roche Diagnostics). Tumor cells were cultured in RPMI 1640 medium (Cellgro) with 10% FBS (Life Technologies), 1 U/ml penicillin, 1 μg/ml streptomycin, and 20 mM HEPES buffer (all from Mediatech).

TIL analysis. C57BL/6 mice (5 mice per group) were inoculated subcutaneously with 5×10^5 B16-OVA tumor cells, and BALB/c mice (5 mice per group) were inoculated subcutaneously with 1×10^5 PD-L1 WT or PD-L1 KO breast tumor cells. Once tumors were established (day 7–10 after tumor injection), tumor tissues were removed and incubated in digestion buffer (RPMI medium containing 5% fetal bovine serum, 0.02% collagenase IV, 0.002% DNase I, and 10 U/ml of heparin) for 40 minutes followed with isolation of lymphocytes. To block the PD-1 pathway, on day 9 after B7-H1 (PD-L1) WT or KO breast cancer cells were injected into BALB/c mice, mice were treated with intratumoral injection of anti-mouse PD-1 antibody (clone G4, Mayo Clinic Antibody Core Facility) or control IgG (catalog BP0091, BioXcell) at 20 μg 3 times for a 3-day interval. On day 2 after last treatment, TILs were isolated for analysis of Bim levels (MFI) in $PD\text{-}1^+CD11a^{hi}CD8^+$ T cells.

Statistics. Nonparametric Mann-Whitney test was used to compare baseline frequencies of Bim^+ cells among $PD\text{-}1^+CD11a^{hi}CD8^+$ T cells and Bim MFI in patients who had disease control (CR or PR) compared with those who had progressive disease at 12 weeks and to compare percent change at first radiographic tumor evaluation (12 weeks) in patients who had CR/PR compared with those who had progressive disease. Change in tumor burden at 12 weeks was assessed by investigators using RECIST 1.1. For patients undergoing fluorodeoxyglucose-PET scanning, assessment of tumor progression was done per existing RECIST guidelines. The correlation of Bim with PD-1, granzyme B, and T-bet was analyzed by Pearson correlation test. Data are presented as mean ± SD. The differences in Bim levels or IFN-γ production and percentages of effector cells between 2 animal groups were mainly analyzed by 2-tailed Mann-Whitney *U* test. Paired 2-tailed Student's *t* test was used to compare the difference of Bim levels between WT and PD-L1 KO tumors growing at the same host mice. All statistical analyses were

performed using GraphPad Prism software 5.0 (GraphPad Software Inc.). A *P* value of less than 0.05 was considered statistically significant.

Study approval. The Mayo Clinic Animal Care and Use Committee approved all animal experiments. Human blood leukocytes were acquired from anonymous donors, who had consented for blood donation, from the Blood Transfusion Center at Mayo Clinic. All patients provided signed informed written consent, and the study was approved by the Mayo Clinic Rochester IRB.

Author contributions

HD and RSD conceived the project and were responsible for research design, data analysis, and drafting the manuscript. SNM, ASM, and SSP contributed to the study design and data analysis and interpretation of data. XL, LC, and SC performed the experiments and data acquisition. LAK and RRM contributed to the study design and clinical data acquisition. SHM helped develop the animal models. MAT and WKN collected and processed specimens. HD and SNM supervised all aspects of the work. MSB contributed to clinical data acquisition. All authors approved the submitted manuscript.

Acknowledgments

We are thankful to Tasuku Honjo and Lieping Chen for providing PD-1 and PD-L1 KO mice, Larry Pease for providing BALB NeuT mice and TUBO cell lines, Richard Vile for B16 and B16-OVA cell lines, Jessica Brandt and Renee Bradshaw for helping to enroll patients, and Wei Zhao for optimizing Bim staining in human T cells. This study was supported by the Cancer Research Institute (to H. Dong), the National Cancer Institute grants R21 CA197878 (to H. Dong and R.S. Dronca) and CTSA KL2 TR000136 (to R.S. Dronca), and in part by NIH/National Institute of Allergy and Infectious Diseases grants R01 AI095239 (to H. Dong) and K12CA090628 (to A.S. Mansfield), and in part by funding from the Mayo Clinic Center for Individualized Medicine (CIM) Biomarker Discovery Program.

Address correspondence to: Haidong Dong, Departments of Urology and Immunology, College of Medicine, Mayo Clinic, 200 First Street SW, Rochester, Minnesota 55905, USA. Phone: 507.284.5482; E-mail: dong.haidong@mayo.edu.

1. Topalian SL, et al. Safety, activity, and immune correlates of anti-PD-1 antibody in cancer. *N Engl J Med*. 2012;366(26):2443–2454.
2. Brahmer JR, et al. Safety and activity of anti-PD-L1 antibody in patients with advanced cancer. *N Engl J Med*. 2012;366(26):2455–2465.
3. Hamid O, et al. Safety and tumor responses with lambrolizumab (anti-PD-1) in melanoma. *N Engl J Med*. 2013;369(2):134–144.
4. Brahmer J, et al. Nivolumab versus Docetaxel in advanced squamous-cell non-small-cell lung cancer. *N Engl J Med*. 2015;373(2):123–135.
5. Motzer RJ, et al. Nivolumab versus Everolimus in advanced renal-cell carcinoma. *N Engl J Med*. 2015;373(19):1803–1813.
6. Powles T, et al. MPDL3280A (anti-PD-L1) treatment leads to clinical activity in metastatic bladder cancer. *Nature*. 2014;515(7528):558–562.
7. Topalian SL, Drake CG, Pardoll DM. Targeting the PD-1/B7-H1(PD-L1) pathway to activate anti-tumor immunity. *Curr Opin Immunol*. 2012;24(2):207–212.
8. Dong H, et al. Tumor-associated B7-H1 promotes T-cell apoptosis: a potential mechanism of immune evasion. *Nat Med*. 2002;8(8):793–800.
9. Weber JS, et al. Lao CD, et al. Nivolumab versus chemotherapy in patients with advanced melanoma who progressed after anti-CTLA-4 treatment (CheckMate 037): a randomised, controlled, open-label, phase 3 trial. *Lancet Oncol*. 2015;16(4):375–384.
10. Robert C, et al. Anti-programmed-death-receptor-1 treatment with pembrolizumab in ipilimumab-refractory advanced melanoma: a randomised dose-comparison cohort of a phase 1 trial. *Lancet*. 2014;384(9948):1109–1117.
11. Hodi S ea. Evaluation of immune-related response criteria (irRC) in patients (pts) with advanced melanoma (MEL) treated with the anti-PD-1 monoclonal antibody MK-3475. *J Clin Oncol*. 2014;32(5s):suppl, abstr 3006.
12. Wolchok JD, et al. Guidelines for the evaluation of immune therapy activity in solid tumors: immune-related response criteria. *Clin Cancer Res*. 2009;15(23):7412–7420.
13. Taube JM, et al. Association of PD-1, PD-1 ligands, and other features of the tumor immune microenvironment with response to anti-PD-1 therapy. *Clin Cancer Res*. 2014; 20(19):5064–5074.
14. Carbognin L, et al. Differential activity of Nivolumab, Pembrolizumab and MPDL3280A according to the Tumor Expression of Programmed Death-Ligand-1 (PD-L1): sensitivity analysis of trials in melanoma, lung and genitourinary cancers. *PLoS One*. 2015;10(6):e0130142.
15. Wolchok JD, et al. Nivolumab plus ipilimumab in advanced melanoma. *N Engl J Med*. 2013;369(2):122–133.
16. Mansfield AS, et al. Heterogeneity of programmed cell death ligand 1 expression in multifocal lung cancer [published online ahead of print December 14, 2015]. *Clin Cancer Res*. doi:10.1158/1078-0432.CCR-15-2246.
17. Dong H, Zhu G, Tamada K, Chen L. B7-H1, a third member of the B7 family, co-stimulates T-cell proliferation and interleu-

kin-10 secretion. *Nat Med*. 1999;5(12):1365–1369.
18. Gibbons RM, et al. B7-H1 limits the entry of effector CD8(+) T cells to the memory pool by upregulating Bim. *Oncoimmunology*. 2012;1(7):1061–1073.
19. Labi V, et al. Deregulated cell death and lymphocyte homeostasis cause premature lethality in mice lacking the BH3-only proteins Bim and Bmf. *Blood*. 2014;123(17):2652–2662.
20. Liu X, et al. Endogenous tumor-reactive CD8 T cells are differentiated effector cells expressing high levels of CD11a and PD-1 but are unable to control tumor growth. *Oncoimmunology*. 2013;2(6):e23972.
21. Gros A, et al. PD-1 identifies the patient-specific CD8(+) tumor-reactive repertoire infiltrating human tumors. *J Clin Invest*. 2014;124(5):2246–2259.
22. Rai D, Pham NL, Harty JT, Badovinac VP. Tracking the total CD8 T cell response to infection reveals substantial discordance in magnitude and kinetics between inbred and outbred hosts. *J Immunol*. 2009;183(12):7672–7681.
23. Gros A, et al. Prospective identification of neoantigen-specific lymphocytes in the peripheral blood of melanoma patients. *Nat Med*. 2016;22(4):433–438.
24. Duraiswamy J, et al. Phenotype, function, and gene expression profiles of programmed death-1(hi) CD8 T cells in healthy human adults. *J Immunol*. 2011;186(7):4200–4212.
25. Hildeman DA, et al. Activated T cell death in vivo mediated by proapoptotic bcl-2 family member bim. *Immunity*. 2002;16(6):759–767.
26. Lopes AR, et al. Bim-mediated deletion of antigen-specific CD8 T cells in patients unable to control HBV infection. *J Clin Invest*. 2008;118(5):1835–1845.
27. Bouillet P, et al. Proapoptotic Bcl-2 relative Bim required for certain apoptotic responses, leukocyte homeostasis, and to preclude autoimmunity. *Science*. 1999;286(5445):1735–1738.
28. Strasser A. The role of BH3-only proteins in the immune system. *Nat Rev Immunol*. 2005;5(3):189–200.
29. Cruz-Guilloty F, et al. Runx3 and T-box proteins cooperate to establish the transcriptional program of effector CTLs. *J Exp Med*. 2009;206(1):51–59.
30. Afonina IS, Cullen SP, Martin SJ. Cytotoxic and non-cytotoxic roles of the CTL/NK protease granzyme B. *Immunol Rev*. 2010;235(1):105–116.
31. Zak KM, et al. Structure of the complex of human programmed death 1, PD-1, and its ligand PD-L1. *Structure*. 2015;23(12):2341–2348.
32. Qi XJ, Wildey GM, Howe PH. Evidence that Ser87 of BimEL is phosphorylated by Akt and regulates BimEL apoptotic function. *J Biol Chem*. 2006;281(2):813–823.
33. Thompson RH, et al. Tumor B7-H1 is associated with poor prognosis in renal cell carcinoma patients with long-term follow-up. *Cancer Res*. 2006;66(7):3381–3385.
34. Larkin J, et al. Combined Nivolumab and Ipilimumab or monotherapy in untreated melanoma. *N Engl J Med*. 2015;373(1):23–34.
35. Daud A, et al. Long-term efficacy of pembrolizumab (pembro; MK-3475) in a pooled analysis of 655 patients (pts) with advanced melanoma (MEL) enrolled in KEYNOTE-001. *J Clin Oncol*. 2015;33:(suppl; abstr 9005).
36. Ludwinski MW, et al. Critical roles of Bim in T cell activation and T cell-mediated autoimmune inflammation in mice. *J Clin Invest*. 2009;119(6):1706–1713.
37. Yu Y, Yu J, Iclozan C, Kaosaard K, Anasetti C, Yu XZ. Bim is required for T-cell allogeneic responses and graft-versus-host disease in vivo. *Am J Blood Res*. 2012;2(1):77–85.
38. Taube JM, et al. Colocalization of inflammatory response with B7-h1 expression in human melanocytic lesions supports an adaptive resistance mechanism of immune escape. *Sci Transl Med*. 2012;4(127):127ra37.
39. Sandalova E, Wei CH, Masucci MG, Levitsky V. Regulation of expression of Bcl-2 protein family member Bim by T cell receptor triggering. *Proc Natl Acad Sci U S A*. 2004;101(9):3011–3016.
40. Kurtulus S, et al. Bcl-2 allows effector and memory CD8$^+$ T cells to tolerate higher expression of Bim. *J Immunol*. 2011;186(10):5729–5737.
41. Rosell R, et al. Erlotinib versus standard chemotherapy as first-line treatment for European patients with advanced EGFR mutation-positive non-small-cell lung cancer (EURTAC): a multicentre, open-label, randomised phase 3 trial. *Lancet Oncol*. 2012;13(3):239–246.
42. Costa C, et al. The impact of EGFR T790M mutations and BIM mRNA expression on outcome in patients with EGFR-mutant NSCLC treated with erlotinib or chemotherapy in the randomized phase III EURTAC trial. *Clin Cancer Res*. 2014;20(7):2001–2010.
43. Karachaliou N, et al. BIM and mTOR expression levels predict outcome to erlotinib in EGFR-mutant non-small-cell lung cancer. *Sci Rep*. 2015;5:17499.